

Probing the Sun's inner core using solar neutrinos: a new diagnostic method

Ilídio Lopes*

CENTRA, Instituto Superior Técnico, 1049-001 Lisboa, Portugal
and

Departamento de Física, Universidade de Évora, 7002-554 Évora, Portugal

(Published in Phys. Rev. D 88, 045006, 7 August 2013)

The electronic density in the Sun's inner core is inferred from the 8B , 7Be and pep neutrino flux measurements of the Super-Kamiokande, SNO and Borexino experiments. We have developed a new method in which we use the KamLAND detector determinations of the neutrino fundamental oscillation parameters: the mass difference and the vacuum oscillation angle. Our results suggest that the solar electronic density in the Sun's inner core (for a radius smaller than 10% of the solar radius) is well above the current prediction of the standard solar model, and by as much as 25%. A potential confirmation of these preliminary findings can be achieved when neutrino detectors are able to reduce the error of the electron-neutrino survival probability by a factor of 15.

I. INTRODUCTION

Traveling close to the speed of light and with a very large mean free path, solar neutrinos provide a unique and powerful tool to study the properties of the plasma in the Sun's core. During the last two decades, the increase in the number of neutrino detectors, accompanied by a significant improvement in the accuracy of the measurements has led to major progress in the research field of neutrino physics.

Among many breakthroughs in solar neutrino physics, two are particularly worth mentioning- due to their relevance for this work. In 2001, the Sudbury Neutrino Observatory (SNO) experiment [1], following in the footsteps of previous neutrinos experiments [e.g. 2], definitely confirmed the neutrino flavor oscillations in vacuum and matter. This theoretical model was first suggested by Pontecorvo [3] to explain oscillations in vacuum, and later extended by Wolfenstein [4], Mikheyev and Smirnov [5] to include the oscillations of neutrinos in matter. This is the reason why this last oscillation mechanism is also called the Mikheyev-Smirnov-Wolfenstein (MSW) effect.

In the following year another important discovery occurred: the Kamiokande Liquid Scintillator Anti-Neutrino Detector (KamLAND) [6] measured the flux of antineutrinos from distant reactors confirming the oscillation nature of neutrinos. Furthermore, KamLAND found that a unique combination of oscillation parameters could explain the neutrino oscillations data, the so-called large mixing angle solution. More significantly, for the first time it was possible to measure the parameters related with the flavor oscillations of neutrinos in vacuum, from a source of neutrinos that is not the Sun. The three-flavor neutrino oscillations based only on KamLAND data analysis [7, 8] give $\Delta m_{21}^2 = 7.49 \pm 0.20 \times 10^{-5} eV^2$ and $\tan^2 \theta_{21} = 0.436 \pm 0.102$. The two-flavor neutrino oscillations data analysis ($\theta_{13} = 0$)

gives identical results, but the value of $\tan^2 \theta_{21}$ increases by 11%.

Once the fundamental parameters of neutrino flavor oscillations are determined independently of the neutrinos coming from the Sun (at least in the case of the KamLAND experiment), it is reasonable to use, or at least to discuss, the possibility of using solar neutrino flux measurements to probe the Sun's interior. Although our understanding of the basic physical mechanisms occurring inside the Sun is quite robust, there is still a certain number of unknown processes in the solar core that neutrinos could help to resolve [see Ref. 9, and references therein]. Furthermore, if we wish to use the Sun as a cosmological tool [e.g., Refs. 10–16] in an identical manner to how neutron stars [e.g., Refs. 17–21] are used to constrain the dark matter particle properties, then this will only be possible if we have reliable methods to diagnose the solar core.

Most of the progress achieved in describing accurately the physical processes occurring in the Sun's interior is owed to helioseismology [e.g., Ref. 2]: the present seismic data allows the determination of the sound-speed and density radial density profiles to be obtained with high accuracy, between the solar surface and the first layers of the nuclear region [22, 23]. Comparing the present Sun's structure as predicted by the standard solar model (SSM) with the helioseismological data, the sound-speed difference is at most of the order of 2% (mainly in the radiative region) and the density difference is of the order of 10% (in the convective zone). The origin of the sound-speed difference is unknown, probably related to some physical mechanisms occurring during the evolution of the star [9], but the density difference has been linked to a poor description of the solar convection [24, 25].

In the last few years, several theoretical models have been put forward to explain this discrepancy between theory and helioseismological data. Most of these proposals are able to reduce the sound-speed difference. Among the various proposals, we choose to mention three of them, which are also validated by stellar observations. This is the case with solar models with no standard pre-main-sequence evolution, like solar evolution models that

* ilidio.lopes@ist.utl.pt; ilopes@uevora.pt

take into account the temporal evolution of the solar internal rotation [26], and solar models for which during a certain period of their pre-main-sequence evolution, the star has its mass changed by a mechanism of mass-loss or accretion [27, 28].

Another physical process that has been recently considered important for Sun-like stars with planetary systems, is the possibility that the star during its formation or even in its pre-main-sequence phase, could have its internal metallicity increased due to the migration of heavy nuclei from the planetary disk towards the core of the protostar [29]. This scenario has been suggested by recent high-precision spectroscopic observations of solar twins with and without planetary systems [30, 31]. In particular, it was found that the former group of stars presents a larger amount of metals in the surface than the latter group. Up to now, how exactly this mechanism operates is still unknown, but it has been shown to be linked to the formation of Earth-like planets. If this process occurs, this could increase significantly the abundances of elements such as carbon, nitrogen and oxygen, increasing the overall metallicity of the stellar interior. Therefore, the amount of heavy elements like carbon, nitrogen and oxygen in the Sun's interior can be well above the values presently measured in the solar photosphere [32]. The observations suggest that stars like the Sun could have a 30% excess of metals in their radiative interior when compared with current values predicted by the standard solar model [2, 9]. Furthermore, the sound-speed difference is reduced to a value qualitatively close to the sound-speed difference obtained with the previous metal abundance measurements [33]. This issue is particularly relevant for the neutrinos produced in the nuclear reactions of the carbon-nitrogen-oxygen (CNO) cycle. If the excess in abundances occurs for Carbon, Nitrogen and Oxygen elements, the neutrino fluxes produced in the CNO cycle will be well above the values predicted by the standard solar model [29].

As shown, several physical mechanisms are concurrent with each other towards reducing the sound-speed difference in the solar interior, but the current solar data (including helioseismology data) do not allow us unequivocally to determine which are the best proposals. A strategy going forward to resolve this issue is to investigate new techniques to diagnose the plasma of the solar interior including the solar inner core. In particular, this will be done by constraining quantities other than the sound-speed profile, such as the electronic density or the plasma density.

Presently, due to the low amount of low-degree acoustic modes, there is still a large uncertainty in the inversion of the sound-speed profile in the solar inner core, and consequently, the seismic diagnostic of this region is quite inaccurate. Even if it is possible to have some information about the sound-speed in this region, our knowledge about the local density is much more uncertain. Naturally, the most reliable hope to probe the density in the Sun's core is to use gravity modes, although their exist-

tence must still be confirmed [34]. The solar neutrinos are a natural alternative for diagnosing the solar interior, provided that the precision in the measurement of neutrino fluxes is obtained with the required accuracy. If this experimental goal is succeeded, it will provide a major contribution for resolving this problem.

A first attempt to obtain the electronic density in the Sun's interior was made by Balantekin *et al.* [35]. In their work, the authors computed the electronic density as an expansion in powers of the local density plasma, under the hypothesis that neutrino oscillations occur with a small-angle MSW solution. The result obtained allows a relatively good analytical representation of the electronic density in most of the radiative region. The method becomes imprecise only in the core of the Sun below 20% of the solar radius.

Finally, it is worth mentioning that there is still some uncertainty on the basic parameters of neutrino oscillations, which in turn can introduce some uncertainty in the total fluxes of neutrinos of different flavors. However, as was pointed out by Bhat *et al.* [36], this effect is much smaller than the MSW effect discussed in this work. In particular, Balantekin and Malkus [37] have studied the impact of the third neutrino oscillation mixing angle in vacuum on the neutrino flavor oscillations related with matter, and have found that the impact was negligible. A review of the properties of the propagation of neutrinos in matter can be found in Balantekin [38].

In this paper, we focus on the inner nuclear region of the Sun ($r \leq 0.1R_{\odot}$), and we will present and discuss a new diagnostic method that constrains the electronic density that comes from current neutrino flux measurements in this region. The method is based in determining the electronic density in the Sun's inner core, as a linear correction to the present values of solar neutrino fluxes obtained for the present standard solar model. What makes this new diagnostic particularly appealing is the possibility of constraining the electronic density at a distance of 5% from the center of the Sun, a very central region which is very difficult to probe by any other methods.

II. THE SOLAR NEUTRINO ENERGY SPECTRUM

Neutrinos are produced in the Sun's interior through several reactions of the nuclear network, usually known as proton-proton (PP) chains and carbon-nitrogen-oxygen (CNO) cycle. Figure 1 shows the neutrino spectra of our standard solar model [39] computed with an updated version of the stellar evolution code CESAM [40]. This version of CESAM has an up-to-date and very refined microscopic physics (equation of state, opacities, nuclear reaction rates, and an accurate treatment of microscopic diffusion of heavy elements), including the solar mixture of Asplund *et al.* [32] and nuclear reaction rates from NACRE Compilation [41, 42]. The solar models are calibrated to

the present solar radius $R_\odot = 6.9599 \times 10^{10}$ cm, luminosity $L_\odot = 3.846 \times 10^{33}$ erg s $^{-1}$, mass $M_\odot = 1.989 \times 10^{33}$ g, and age $t_\odot = 4.54 \pm 0.04$ Gyr [e.g. Ref. 2]. The models are required to have a fixed value of the photospheric ratio of metal abundance over hydrogen abundance in agreement with the used solar mixture. The total neutrino fluxes (on Earth) predicted by this model are the following: $\phi(pep) = 1.4 \cdot 10^8$, $\phi(^7Be) = 4.7 \cdot 10^9$, $\phi(^8B) = 5.3 \cdot 10^6$, $\phi(^{13}N) = 5.3 \cdot 10^8$, $\phi(^{15}O) = 4.5 \cdot 10^8$, $\phi(^{17}F) = 5.0 \cdot 10^6$ and $\phi(pp) = 5.9 \cdot 10^{10}$, in units of cm $^{-2}$ s $^{-1}$. This solar model is in agreement with the most current helioseismology data and is identical to others published in the literature [e.g., Refs. 26–28, 43]. The neutrino fluxes of 8B , 7Be and pep are in agreement with the current solar neutrino experiments. The new NACRE table [41] presents a set of S factors slightly different of previous ones [42], but with a smaller error bar. Therefore, the 8B , 7Be and pep total neutrino fluxes are almost the same ones found on previous predictions, the differences are mainly due to the change of S factors of few nuclear reactions like $^3He(^3He, 2p)^4He$ and $^7Be(p, \gamma)^8B$. Nevertheless, the standard solar model computed with this new set of laboratory cross-section measurements [41] predicts solar neutrino fluxes in excellent agreement with experimental data [44]. Moreover, the impact of this update of the NACRE table on the Sun's core electronic density is negligible, because the ratios of neutrino flavor fluxes are almost independent of the total neutrino flux for each neutrino source.

Figure 2 shows the different neutrino emission sources inside the Sun. The nuclear reactions are ordered inside the Sun according to the temperature required for the fusion reaction between reacting nuclei to occur. Naturally, the nuclear reactions between heavy nuclei are located nearer the center, than reactions between lighter nuclei. In Fig. 2 we show the electron-neutrino source function $\Phi(r)$ related to the electron-neutrinos produced in the PP chain (pp , pep , 8B and 7Be) and CNO cycle (^{13}N , ^{15}O , ^{17}F) nuclear reactions.

The neutrino sources produced by the nuclear reactions of the PP chain are located between the center and 30% of the solar radius. The pp neutrino source extends from the center up to 30% of the solar radius with its maximum located at 10% of the solar radius. The other PP chain neutrino sources are pep , 7Be and 8B and have emission shell with widths of 22%, 18% and 10% respectively, and maximums occurring at 8.6%, 5.8% and 4.5% of the solar radius, respectively. In particular, it is worth noticing that the pp and pep nuclear reactions are strongly dependent on the total luminosity of the star. Similarly, the neutrino sources related with the CNO cycle of nuclear reactions (cf. Fig. 2), ^{15}O , ^{17}F and ^{13}N neutrinos occur in emission shells with a width of 16% of the solar radius. The maximum neutrino production of these sources occurs at 5% of the solar radius. ^{13}N neutrinos have a second emission shell located between 12% and 25% of the Sun's radius with its maximum occurring at 16% of the solar radius.

It is important to note that an increase or decrease of the temperature in the core of the Sun (caused by the presence of some known or unknown physical process) does not change much the location of the neutrino emission region $\Phi(r)$, even if the total neutrino fluxes change significantly (cf. Fig 2). This is due to the strong dependence of neutrino nuclear reactions on the temperature.

In the case of solar models for which the central temperature is changed by a few percent, the neutrino emission regions (i.e., the 8B , 7Be and pep neutrino emission regions among others) does not change much, although the total neutrino fluxes are strongly affected. The position of the maximum of $\Phi(r)$ of the different neutrino sources changes by less than 1%.

III. NEUTRINO FLAVOR OSCILLATIONS

The theory of neutrino flavor oscillations [i.e., Ref. 45] describes the propagation of neutrinos in space [3] and the interaction of neutrinos with matter [4, 5]. Yuksel [46] showed that the survival probability of solar neutrinos calculated in a model with two neutrino flavor oscillations or three neutrino flavor oscillations have very close values.

In the Sun, the electron-neutrino survival or appearance probabilities depend only on three fundamental oscillation parameters: the mass difference Δm_{12} and the angles θ_{21} and θ_{13} . In the absence of the MSW effect caused by the Earth's globe, the survival probability during the day of a three-flavor neutrino oscillation can be reduced to a modified two-flavor neutrino oscillation model that is accurately described as

$$P_{\nu_e}(E_\nu, r) = \cos^4 \theta_{13} P_{2\nu_e}(E_\nu, r) + \sin^4 \theta_{13}, \quad (1)$$

where E_ν is the energy of the neutrino and $P_{2\nu_e}(E_\nu, r)$ is the probability in the case of a two-flavor oscillation model [e.g., Refs. 7, 45, 47]. $P_{2\nu_e}(E_\nu, r)$ is given by

$$P_{2\nu_e}(E_\nu, r) = \frac{1}{2} + \frac{1}{2} \cos(2\theta_{21}) \cos(2\theta_m) \quad (2)$$

where θ_m is the mixing angle at the production source inside the Sun. In the derivation of this formula it was assumed that the first-order correction to the propagation of neutrinos in matter is valid once the adiabatic condition is verified in the radiative region of the solar interior [47, 48]. The phase θ_m is the most important term in this analysis, since it depends on the electron density of the Sun's core. The mixing angle θ_m is given by

$$\sin(2\theta_m) = \frac{\sin(2\theta_{12})}{\sqrt{(V_m - \cos(2\theta_{12}))^2 + \sin^2(2\theta_{12})}}, \quad (3)$$

where V_m is a function of solar radius. The values of Δm_{12}^2 and θ_{21} can be solely determined from neutrino experiments (not using the neutrinos coming from the Sun), such as the KamLAND reactor experiment [6]. V_m is a function of solar plasma density, given by

$$V_m(E_\nu, r) = 2\sqrt{2}G_f n_e(r) E_\nu \cos^2(\theta_{13})/\Delta m_{21}, \quad (4)$$

where G_f is the Fermi constant and $n_e(r)$ is the electron density of plasma. The electron density $n_e(r) = N_o \rho(r)/\mu_e(r)$, where $\mu_e(r)$ is the mean molecular weight per electron, $\rho(r)$ the density of matter in the solar interior and N_o the Avogadro's number.

The radial neutrino emission profile of electron neutrinos is specific for each nuclear reaction (cf. Fig. 2). It follows that the average survival probability of electron neutrinos for each of the emission neutrino sources, $\langle P_{\nu_e}(E_\nu) \rangle$ is given by

$$\langle P_{\nu_e}(E_\nu) \rangle = A^{-1} \int P_{\nu_e}(E_\nu, r) \Phi(r) 4\pi \rho(r) r^2 dr \quad (5)$$

where $A = \int \Phi(r) 4\pi \rho(r) r^2 dr$ is a normalization constant. In the following $\langle \dots \rangle$ defines the $\Phi(r)$ weight averaged of a certain quantity, as defined in the previous equation.

The electron-neutrino survival probability functions $\langle P_{\nu_e}(E_\nu) \rangle$ for different nuclear reactions are shown in Fig. 3. The survival probabilities of electron-neutrinos were computed by using the fundamental parameters of solar neutrino oscillations in vacuum namely Δm_{12} and θ_{12} , as determined by the KamLAND experiment [7]. Although the contribution related to θ_{13} is minor, we take its contribution into account by choosing $\theta_{13} = 9$ deg, a value that is in agreement with current experimental measurements, $8.96^{+0.45}_{-0.51}$ deg [49] and $9.06^{+0.50}_{-0.57}$ deg [50]. Furthermore, Balantekin and Malkus [37] have shown that the electron-neutrino survival probability functions are not very sensitive to the mixing θ_{13} for the neutrino energy range where the MSW effect is dominant, at least in the energy range where the neutrino flux measurements are taken.

Since electron neutrinos are produced in nuclear reactions located at different distances from the center, there is a clear differentiation between the different survival probability curves (cf. Fig. 3). Nevertheless, for neutrinos with low or high energy, these curves become indistinguishable, as low-energy neutrinos are affected only by vacuum fluctuations, and high-energy neutrinos are affected by a cumulative effect of vacuum oscillations and matter oscillations. It is worth noticing that the possibility of observing the MSW effect on solar neutrinos is limited, as the neutrino flavor oscillations induced by matter depend on the neutrino emission spectrum (cf. Fig. 1) and on the location of the neutrino source in the Sun's core (cf. Fig. 2). The parts of the survival probability of electron neutrinos that can be measured by solar neutrino experiments are shown in Fig. 3. In particular, we notice that the 8B neutrino flavor oscillation is strongly dependent on the MSW effect, specially for neutrinos with a higher energy. However, the 7Be neutrino flux is much less dependent on the MSW effect, particularly the 7Be neutrino flux corresponding to the line of lower energy. Similarly, the pep neutrino flux is also weakly dependent on the MSW effect. Accordingly, the constraint obtained in the electronic density from the 8B neutrino flux measurement is much more

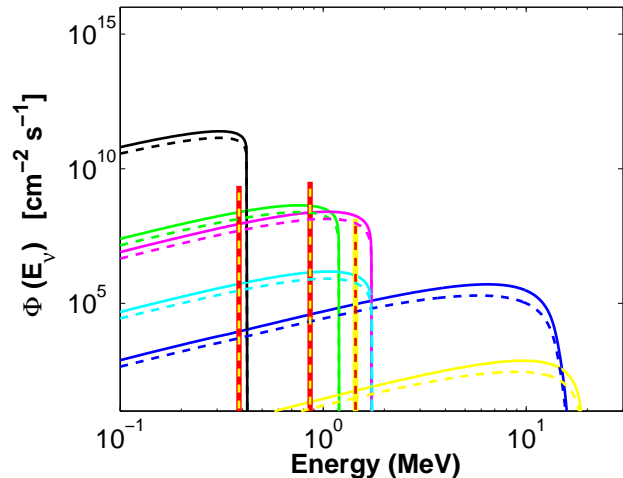


FIG. 1. The solar neutrino energy spectrum predicted by our standard solar model. The solid curves correspond to the total (electron-flavor) neutrino fluxes produced in the various nuclear reactions of the proton-proton chains and carbon-nitrogen-oxygen cycle. The dashed curves correspond to electron-neutrino fluxes of the various nuclear reactions after neutrino flavor conversion. The color curves define the following neutrino sources from the proton-proton chain reactions: 8B (blue curve), 7Be (two red-yellow lines), pep (yellow-red line), hep (yellow curve) and pp (black curve); and the following neutrino sources from the carbon-nitrogen-oxygen: ${}^{13}N$ (green curve), ${}^{15}O$ (magenta curve) and ${}^{17}F$ (cyan curve). The neutrino fluxes from continuum nuclear sources are given in units of $\text{cm}^{-2}\text{s}^{-1}\text{MeV}^{-1}$. The line neutrino fluxes are given in $\text{cm}^{-2}\text{s}^{-1}$.

reliable than the constraint obtained from 7Be and pep neutrino flux measurements (cf. Fig. 3). Furthermore, it is worth noticing a second-order effect. The conversion of electron neutrinos due to matter oscillations depends on the local electron density $n_e(r)$: a decrease of the central density of $n_e(r=0)$ moves all the $\langle P_{\nu_e}(E_\nu) \rangle$ of different neutrino sources to the right, and a rapid variation of $n_e(r)$ (possibly caused by a rapid variation of density) with the radius increases the distance between the consecutive $\langle P_{\nu_e}(E_\nu) \rangle$ curves (cf. Fig. 3).

Once the fundamental parameters of solar neutrino oscillations in vacuum are known and determined independently from solar neutrino fluxes, in principle, the probability of survival of electron-flavor solar neutrinos can be used to infer the radial electronic density profile in different locations of the solar core. By perturbation analysis of Eqs. (1-5), the value of the electronic n is determined for each value of the survival probability of electron neutrinos obtained from the experimental neutrino data [39]. The procedure is as follows: for neutrinos of a given energy E_ν , the electronic density correction Δn is computed from the standard solar model electronic density n_o as $\Delta n/n_o = \beta_o \Delta P/P_o$, with $\Delta P = \bar{P} - P_o$ where P_o and \bar{P} are the survival probabilities of electron neutrinos obtained from the standard solar model and experimental

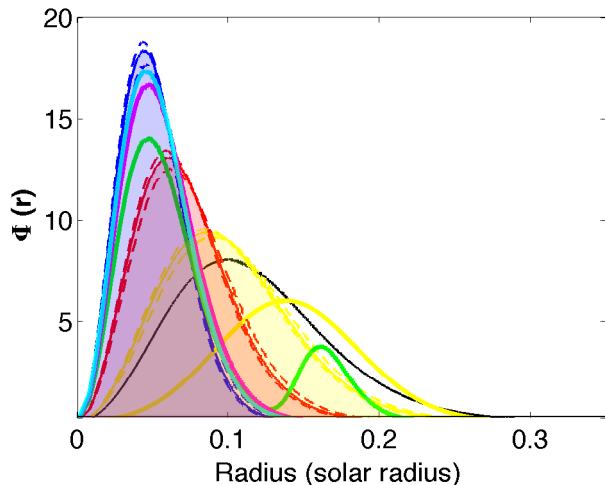


FIG. 2. The electron-neutrino fluxes produced in the various nuclear reactions. The $\Phi(r)$ for which neutrino fluxes have been measured experimentally (8B , 7Be and pep) are indicated with a shaded area. If the central temperature of the standard solar model changes by +2.5% (−4%) and density changes accordingly (+7.4% and −12.7%) to keep the energetic balance, the neutrino fluxes change by +70% (−60%) for 8B , by 30% (−38%) for the 7Be neutrino emission lines and by 13% (−20%) for the pep emission line. The function $\Phi(r)$ for these two cases is indicated by dashed curves. The color scheme is the same as for Fig. 1. In particular, 7Be (two red-yellow lines) and pep (yellow-red line) in Fig. 1 correspond this figure’s red and yellow shaded areas, respectively.

data. β_o is a coefficient computed from the standard solar model data. It follows that the new value of electronic density, \bar{n}_e is obtained as $\bar{n}_e = n_o + \Delta n$. Figure 4 shows the inverted electronic density values obtained from the survival probability of electron neutrinos computed from experimental data.

IV. SOLAR NEUTRINO FLUXES

Usually, the fluxes of the different neutrino flavors are represented by Φ_t for the total neutrino flux, Φ_e for the electron-neutrino flux, and $\Phi_{\tau\mu}$ for the nonelectron flavor component of neutrinos, corresponding to the experimentally indistinguishable flavors of τ and μ neutrinos [45]. It follows that $\Phi_t = \Phi_e + \Phi_{\tau\mu}$. Such quantities are computed from the measured neutrino fluxes that result from the interaction of neutrinos with the detector, which occur through three different interaction processes. As for the charged-current reaction (CC) of neutrinos with a deuterium nucleus and the elastic scattering (ES) of neutrinos off electrons, both processes are observed through the detection of the Cherenkov light produced by electrons in the heavy water. A third process known as neutral-current (NC) reaction is observed via the detection of neutrons. Conveniently, such neu-

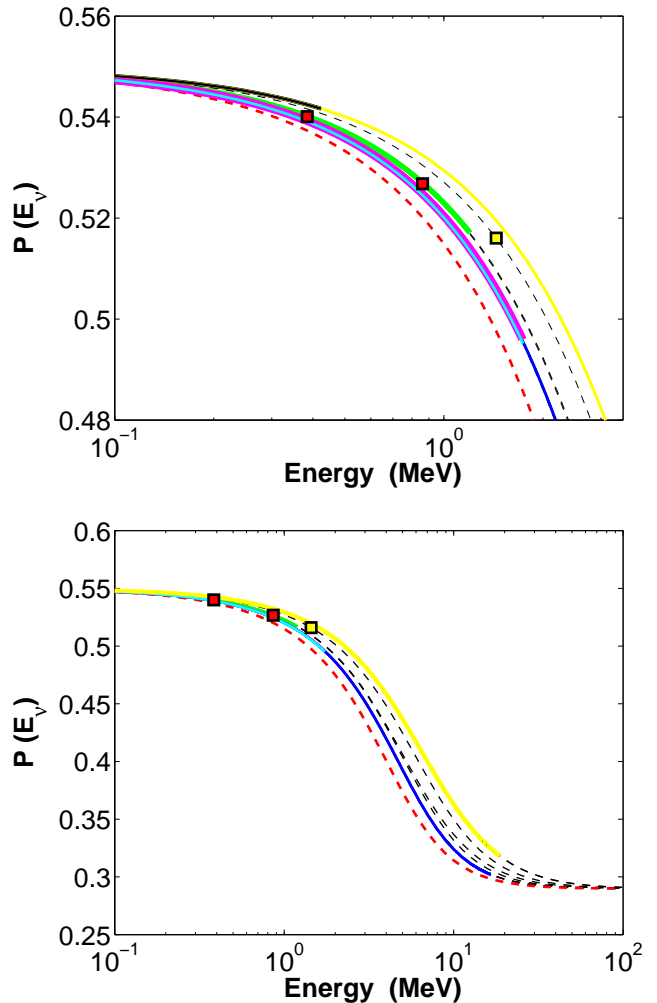


FIG. 3. The survival probability of electron-neutrinos in function of the neutrino energy. The reference curve (red dashed curve) defines the survival probability of electron-neutrinos in the centre of the Sun. The colored parts of the curves indicate the energy range of neutrinos produced in the Sun’s core for each nuclear reaction (cf. Fig. 1).

trino fluxes are called Φ_{CC} , Φ_{ES} and Φ_{NC} . Φ_t is determined as $\Phi_t = \Phi_{NC}$, once that the neutral-current reaction is sensitive to all flavors of neutrinos. The flux of electron-neutrinos is measured by the charged-current reaction $\Phi_e = \Phi_{CC}$, or alternatively it can be measured by the neutrino-electron scattering (ES), for which Φ_e is computed as $\Phi_e = 1.2\Phi_{ES} - 0.20\Phi_{NC}$.

Among current solar neutrino experiments, the measurements of 8B neutrino flavors are the most compelling because for 8B neutrinos, unlike in the case of 7Be and pep neutrinos [51–53], the measurements allow the computation of Φ_t and Φ_e for different and independent solar experiments. Furthermore, 8B neutrino flux is much more sensitive to the density stratification of the solar core— i.e., the neutrino flavor oscillation induced by the

TABLE I. 8B neutrino fluxes and electron-neutrino survival probabilities

Experiment [Φ_{NC}] $10^6 \text{ cm}^{-2}\text{s}^{-1}$	Φ_{CC} or Φ_{ES} $10^6 \text{ cm}^{-2}\text{s}^{-1}$	Φ_e $10^6 \text{ cm}^{-2}\text{s}^{-1}$	P_{ν_e}
SNO(Phase III) 5.54 ± 0.69			
SNO (Phase III) ^a	$CC:1.67 \pm 0.12$	1.67 ± 0.12	0.30 ± 0.04
SNO (Phase II) ^b	$CC:1.76 \pm 0.14$	1.76 ± 0.14	0.32 ± 0.05
Borexino ^c	$ES:2.4 \pm 0.5$	1.77 ± 0.62	0.32 ± 0.12
SK (Phase III) ^d	$ES:2.32 \pm 0.09$	1.67 ± 0.18	0.30 ± 0.05
SNO (En. NC) 5.21 ± 0.65			
SNO (Phase III)	$CC:1.67 \pm 0.12$	1.67 ± 0.12	0.32 ± 0.05
SNO (Phase II)	$CC:1.76 \pm 0.14$	1.76 ± 0.14	0.34 ± 0.05
Borexino	$ES:2.4 \pm 0.5$	1.84 ± 0.61	0.35 ± 0.13
SK (Phase III)	$ES:2.32 \pm 0.09$	1.74 ± 0.17	0.33 ± 0.05
Mean Value	–	–	0.32 ± 0.20

^a Aharmim *et al.* [54]

^b Aharmim *et al.* *et al.* [55]

^c Bellini *et al.* *et al.* [56]

^d Abe *et al.* *et al.* [57]

MSW effect, than other sources of neutrino fluxes such as 7Be and pep neutrinos. This allows us to make an estimation of the survival probability of electron-neutrino flavors independent of solar models and neutrino oscillation models (see Table I). $\Phi_t({}^8B)$ is estimated by the Sudbury Neutrino Observatory (SNO phase III) experiment [54] from $\Phi_{NC}({}^8B)$, a value 7% larger than the previous SNO measurement [58]. The SNO Collaboration have performed another measurement [59] of $\Phi_{NC}({}^8B)$ by enhancing the sensitivity of heavy water to neutral current interaction (En. NC).

In Table I we show the electron-neutrino flux $\Phi_e({}^8B)$ estimated from the SNO, Super-Kamiokande and Borexino measurements [55–57]. Although the errors in most of the neutrino-measured fluxes are still quite significant, it is encouraging to observe that the different experiments lead to quite identical values of $\Phi_e({}^8B)$. The $\Phi_{ES}({}^8B)$ computed in the case of SNO phase III predicts a value 4% lower than that in the case of SNO En. NC. The survival probability of electron-neutrinos $P_{\nu_e}({}^8B)$ was computed as the ratio $\Phi_e({}^8B)/\Phi_t({}^8B)$ [60]. The error is obtained by adding up the errors quadratically. The values of $P_{\nu_e}({}^8B)$ are quite similar for all experiments with a difference smaller than 17% (Cf. Table I). In particular, the value of the Borexino data (SNO phase III), $P_{\nu_e}({}^8B) = 0.32 \pm 0.12$ is 9% higher than the estimation made by the Borexino Team [56], which obtained a value $P_{\nu_e}({}^8B) = 0.29 \pm 0.1$ at the mean energy of 8.9 MeV. The averaged value of all the experiments $P_{\nu_e}({}^8B)$ is estimated to be 0.32 ± 0.20 . Figure 4 shows the *inverted* electronic density \bar{n}_e ($\equiv n_e(\bar{r})$) at different locations of the solar radius, computed as described in the previous section. The theoretical value P_o was estimated for neu-

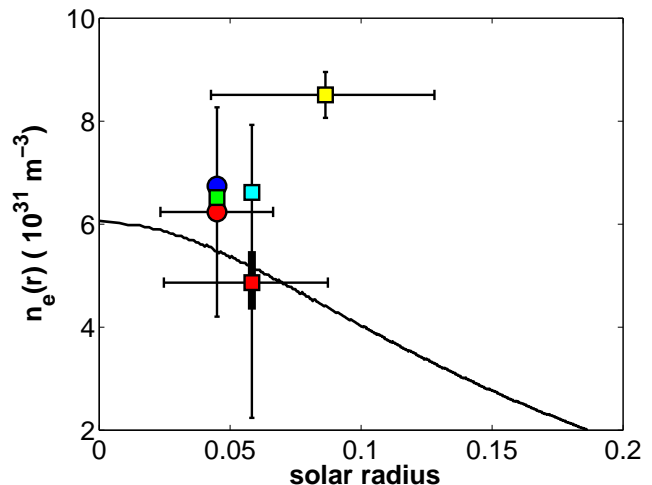


FIG. 4. The core of the Sun: the radial profile of electronic density (black continuous curve). The points shown correspond to the values of the electronic density *inverted*, $n_e(\bar{r})$, for the values of \bar{r} , $0.045 R_\odot$, $0.058 R_\odot$ and $0.086 R_\odot$ computed from the survival probability of electron neutrinos for 8B , 7Be and pep neutrino fluxes (see Table I): (a) 8Be neutrino flux - averaged $P_{\nu_e}({}^8B)$ (red sphere), $P_{\nu_e}({}^8B) = 0.32 \pm 0.05$ (SNO), $P_{\nu_e}({}^8B) = 0.32 \pm 0.12$ (Borexino, green square). (b) 7Be and pep neutrino fluxes (Borexino experiment), (i) The $P_{\nu_e}(pep) = 0.62 \pm 0.17$ (yellow square) [53], (ii) The $P_{\nu_e}({}^7Be) = 0.52^{+0.07}_{-0.06}$ (red square) and $P_{\nu_e}({}^7Be) = 0.56^{+0.10}_{-0.10}$ (cyan square) [51, 52]. The electronic densities inverted from the 8B (red circle) and pep (yellow square) neutrino fluxes were computed assuming that the current vertical errors of $P_{\nu_e}({}^8B)$ and $P_{\nu_e}(pep)$ were reduced by a factor 15. In the case of the 7Be (red square) neutrino flux, this was computed using the real vertical error bar – the thicker bar here corresponds to a reduction of the current error by a factor of 5.

trinos with energy above 5 MeV in the case of 8B neutrinos, and for the values of 0.862 MeV and 1.44 MeV for 7Be and pep neutrinos. In Fig 4, for reasons of clarity, the error bars are shown only in three cases. In all these data points, the length of the *horizontal error bar* of each inverted data point \bar{n}_e (of a specific \bar{r}) defines the radial interval where 68.2% (equivalent to one σ , in a normal distribution) of the neutrino flux is produced.

The mean value of $P_{\nu_e}({}^8B)$ and most of the individual values suggest that the electronic density in the core of the Sun is at least 25% higher than in the current solar model (cf. Table I and Fig. 4). The high value of $P_{\nu_e}(pep)$ obtained by the Borexino Team reinforces the high value of $n_e(r)$ in the core. Although the present value of $P_{\nu_e}({}^7Be)$ is in agreement with the standard solar model, the previous determination $P_{\nu_e}({}^7Be)$ also suggests a high value of $n_e(r)$ in the core. Nevertheless, it should be noticed that both electronic density values obtained from pep and 7Be survival electron-neutrino probabilities, depend on the solar model (contrarily to 8B), and therefore have a limited diagnostic capability.

A potential confirmation of our findings can be achieved as the experimental error in the neutrino measurements decreases and levels of accuracy significantly increase. As per Fig. 4, a clear insight will be possible if the error in the determination of the electron-neutrino survival probability obtained from the present measurements can be reduced by a factor of 15.

V. SUMMARY AND CONCLUSION

We show that if the fundamental parameters of neutrino oscillations are determined from Earth's neutrino detector flux measurements, as per the KamLAND experiment, then the solar neutrino fluxes can be used to invert the electronic density in the Sun's inner core. In this work we have developed a new method to infer the electronic density based in this principle. The method consists in determining the *real* electronic density of the solar core (in function of the radius) as a small correction to the electronic density predicted by the standard solar model.

All the observed neutrino fluxes, i.e., the 8B , 7Be and pep neutrino fluxes have neutrino emission sources located within 10% of the solar radius. Although the accuracy of the current neutrino flux measurements is low, we have found that a significant improvement in the accuracy of these measurements will allow the determination of the electronic density in the Sun's inner core with an

error smaller than a few percent. In particular, the reduction of the error bar of the 7Be electron-neutrino survival probability by a factor 5, allows the determination of the electronic density with an error of 3% (cf. Fig. 4). The measurements of hep , ^{13}N , ^{15}O and ^{17}F neutrino fluxes will also contribute significantly to improve the quality of inversion of the electronic density in the Sun's core. In particular 8B and hep high-energy neutrino fluxes are very sensitive to matter oscillations (cf. Fig. 3). Therefore accurate measurements of these neutrino fluxes will also put stringent constraints to the electronic density in the Sun's core.

This diagnostic of the electronic density of the Sun's inner core combined with the accurate determination of the abundances of heavy elements such as carbon, nitrogen and oxygen from the neutrino fluxes produced in the CNO cycle provides presently the best way to probe the physics of the Sun's inner core. This possibility will become feasible with the upgrade of experiments such as Borexino and the Sudbury Neutrino Observatory (SNO+) [61], as well as the new solar neutrino detector Low Energy Neutrino Astrophysics (LENA) [62].

ACKNOWLEDGMENTS

This work was supported by grants from Fundação para a Ciência e Tecnologia and Fundação Calouste Gulbenkian.

-
- [1] Q. R. Ahmad, *et al.* Measurement of the Rate of $\nu_e + d \rightarrow p + p + e$ - Interactions Produced by 8B Solar Neutrinos at the Sudbury Neutrino Observatory. *Physical Review Letters*, 87(7):71301, August 2001.
- [2] Sylvaine Turck-Chieze and Sébastien Couvidat. Solar neutrinos, helioseismology and the solar internal dynamics. *Reports on Progress in Physics*, 74(8):6901, August 2011.
- [3] B. Pontecorvo. Mesonium and Antimesonium. *Soviet Journal of Experimental and Theoretical Physics*, 6:429, 1958.
- [4] L. Wolfenstein. Neutrino oscillations in matter. *Physical Review D*, 17(9):2369–2374, May 1978.
- [5] S. P. Mikheyev and A. Yu. Smirnov. Resonant amplification of ν oscillations in matter and solar-neutrino spectroscopy. *Il Nuovo Cimento C*, 9(1):17–26, January 1986.
- [6] K. Eguchi, *et al.* First Results from KamLAND: Evidence for Reactor Antineutrino Disappearance. *Physical Review Letters*, 90(2):21802, January 2003.
- [7] A. Gando, *et al.* Constraints on θ_{13} from a three-flavor oscillation analysis of reactor antineutrinos at KamLAND. *Phys Rev D*, 83(5):52002, March 2011.
- [8] S. Abe, *et al.* Precision Measurement of Neutrino Oscillation Parameters with KamLAND. *Physical Review Letters*, 100(2):221803, June 2008.
- [9] Sylvaine Turck-Chieze and Ilídio Lopes. Solar-stellar astrophysics and dark matter. *Research in Astronomy and Astrophysics*, 12(8):1107–1138, August 2012.
- [10] Ilídio Lopes and Joseph Silk. Solar Neutrino Physics: Sensitivity to Light Dark Matter Particles. *The Astrophysical Journal*, 752(2):129, June 2012.
- [11] Ilídio Lopes and Joseph Silk. Neutrino Spectroscopy Can Probe the Dark Matter Content in the Sun. *Science*, 330(6):462, October 2010.
- [12] Ilídio Lopes and Joseph Silk. Probing the Existence of a Dark Matter Isothermal Core Using Gravity Modes. *The Astrophysical Journal Letters*, 722(1):L95–L99, October 2010.
- [13] Marco Taoso, Fabio Iocco, Georges Meynet, Gianfranco Bertone, and Patrick Eggenberger. Effect of low mass dark matter particles on the Sun. *Physical Review D*, 82(8):83509, October 2010.
- [14] Daniel T. Cumberbatch, Joyce A. Guzik, Joseph Silk, L. Scott Watson, and Stephen M. West. Light WIMPs in the Sun: Constraints from helioseismology. *Physical Review D*, 82(1):103503, November 2010.
- [15] Ilídio P. Lopes, Joseph Silk, and Steen H. Hansen. Helioseismology as a new constraint on supersymmetric dark matter. *Monthly Notices of the Royal Astronomical Society*, 331(2):361–368, March 2002.
- [16] Ilídio P. Lopes and Joseph Silk. Solar Neutrinos: Probing the Quasi-isothermal Solar Core Produced by Supersymmetric Dark Matter Particles. *Physical Review Letters*, 88(1):151303, April 2002.

- [17] Chris Kouvaris. Limits on Self-Interacting Dark Matter from Neutron Stars. *Physical Review Letters*, 108(19):191301, May 2012.
- [18] Chris Kouvaris and Peter Tinyakov. Constraining asymmetric dark matter through observations of compact stars. *arXiv*, 83(8):83512, April 2011.
- [19] Chris Kouvaris and Peter Tinyakov. Excluding Light Asymmetric Bosonic Dark Matter. *Physical Review Letters*, 107(9):91301, August 2011.
- [20] Chris Kouvaris and Peter Tinyakov. Can neutron stars constrain dark matter? *Physical Review D*, 82(6):63531, September 2010.
- [21] Chris Kouvaris and Peter Tinyakov. On (Not)-Constraining Heavy Asymmetric Bosonic Dark Matter. *arXiv.org*, page 4075, December 2012.
- [22] Sarbani Basu, William J. Chaplin, Yvonne Elsworth, Roger New, and Aldo M. Serenelli. Fresh Insights on the Structure of the Solar Core. *The Astrophysical Journal*, 699(2):1403–1417, July 2009.
- [23] S. Turck-Chieze, S. Basu, A. S. Brun, J. Christensen-Dalsgaard, A. Eff-Darwich, I. Lopes, F. Perez Hernandez, G. Berthomieu, J. Provost, R. K. Ulrich, F. Baudin, P. Boumier, J. Charra, A. H. Gabriel, R. A. Garcia, G. Grec, C. Renaud, J. M. Robillot, and T. Roca-Cortes. First View of the Solar Core from GOLF Acoustic Modes. *Solar Physics*, 175(2):247–265, October 1997.
- [24] William P. Abbett, Michelle Beaver, Barry Davids, Dali Georgobiani, Pamela Rathbun, and Robert F. Stein. Solar Convection: Comparison of Numerical Simulations and Mixing Length Theory. *Astrophysical Journal v.480*, 480:395, May 1997.
- [25] Åke Nordlund, Robert F. Stein, and Martin Asplund. Solar Surface Convection. *Living Reviews in Solar Physics*, 6:2, April 2009.
- [26] S. Turck-Chieze, A. Palacios, J. P. Marques, and P. A. P. Nghiem. Seismic and Dynamical Solar Models. I. The Impact of the Solar Rotation History on Neutrinos and Seismic Indicators. *The Astrophysical Journal*, 715(2):1539–1555, June 2010.
- [27] Joyce Ann Guzik and Katie Mussack. Exploring Mass Loss, Low-Z Accretion, and Convective Overshoot in Solar Models to Mitigate the Solar Abundance Problem. *The Astrophysical Journal*, 713(2):1108–1119, April 2010.
- [28] Aldo M. Serenelli, W. C. Haxton, and Carlos Pena-Garay. Solar Models with Accretion. I. Application to the Solar Abundance Problem. *The Astrophysical Journal*, 743(1):24, December 2011.
- [29] Ilídio Lopes and Joseph Silk. Planetary influence on the young Sun’s evolution: the solar neutrino probe. *submitted for publication*, pages 1–8, June 2013.
- [30] J. Meléndez, M. Asplund, B. Gustafsson, and D. Yong. The Peculiar Solar Composition and Its Possible Relation to Planet Formation. *The Astrophysical Journal Letters*, 704(1):L66–L70, October 2009.
- [31] I. Ramirez, J. Meléndez, and M. Asplund. Accurate abundance patterns of solar twins and analogs. Does the anomalous solar chemical composition come from planet formation? *Astronomy and Astrophysics*, 508(1):L17–L20, December 2009.
- [32] Martin Asplund, Nicolas Grevesse, A. Jacques Sauval, and Pat Scott. The Chemical Composition of the Sun. *Annual Review of Astronomy and Astrophysics*, 47(1):481–522, September 2009.
- [33] N. Grevesse and A. J. Sauval. Standard Solar Composition. *Space Science Reviews*, 85(1):161–174, May 1998.
- [34] S. Turck-Chieze, R. A. Garcia, S. Couvidat, R. K. Ulrich, L. Bertello, F. Varadi, A. G. Kosovichev, A. H. Gabriel, G. Berthomieu, A. S. Brun, I. Lopes, P. Palme, J. Provost, J. M. Robillot, and T. Roca-Cortes. Looking for Gravity-Mode Multiplets with the GOLF Experiment aboard SOHO. *The Astrophysical Journal*, 604(1):455–468, March 2004.
- [35] A. B. Balantekin, J. F. Beacom, and J. M. Fetter. Matter-enhanced neutrino oscillations in the quasi-adiabatic limit. *Physics Letters B*, 427(3):317–322, May 1998.
- [36] C. M. Bhat, P. C. Bhat, M. Paterno, and H. B. Prosper. Study of the Solar Neutrino Survival Probability. *Physical Review Letters*, 81(2):5056–5059, December 1998.
- [37] A. B. Balantekin and A. Malkus. Solar neutrino matter effects redux. *Physical Review D*, 85(1):13010, January 2012.
- [38] A. B. Balantekin. Neutrino propagation in matter. *Physics Reports*, 315:123–135, July 1999.
- [39] Ilídio Lopes and Sylvaine Turck-Chieze. Solar Neutrino Physics Oscillations: Sensitivity to the Electronic Density in the Sun’s Core. *The Astrophysical Journal*, 765(1):14, March 2013.
- [40] P. Morel. CESAM: A code for stellar evolution calculations. *A & A Supplement series*, 124:597–614, September 1997.
- [41] E. G. Adelberger, *et al.* Solar fusion cross sections. II. The pp chain and CNO cycles. *Review of Modern Physics*, 83(1):195–246, January 2011.
- [42] C. Angulo, *et al.* A compilation of charged-particle induced thermonuclear reaction rates. *Nuclear Physics A*, 656(1):3–183, August 1999.
- [43] Aldo M. Serenelli, Sarbani Basu, Jason W. Ferguson, and Martin Asplund. New Solar Composition: The Problem with Solar Models Revisited. *The Astrophysical Journal Letters*, 705(2):L123–L127, November 2009.
- [44] Aldo Serenelli, Carlos Pena-Garay, and W. C. Haxton. Using the standard solar model to constrain solar composition and nuclear reaction S factors. *Physical Review D*, 87(4):43001, February 2013.
- [45] Samoil Bilenky. *Introduction to the Physics of Massive and Mixed Neutrinos*, Lecture Notes in Physics, Volume 817. ISBN 978-3-642-14042-6. Springer-Verlag Berlin Heidelberg, 2010.
- [46] A. B. Balantekin and H. Yuksel. Constraints on Neutrino Parameters from Neutral-Current Solar Neutrino Measurements. *arXiv.org*, (1):113002, September 2003.
- [47] L. Landau and L. Rosenkewitsch. Über die Theorie des elektrischen Durchschlages von A. Joffé. *Zeitschrift für Physik*, 78(11-12):847–848, November 1932.
- [48] Clarence Zener. Non-Adiabatic Crossing of Energy Levels. *Royal Society of London Proceedings Series A*, 137:696–702, September 1932.
- [49] G. L. Fogli, E. Lisi, A. Marrone, D. Montanino, A. Palazzo, and A. M. Rotunno. Global analysis of neutrino masses, mixings, and phases: Entering the era of leptonic CP violation searches. *Physical Review D*, 86(1):13012, July 2012.
- [50] D. V. Forero, M. Tórtola, and J. W. F. Valle. Global status of neutrino oscillation parameters after Neutrino-2012. *Physical Review D*, 86(7):73012, October 2012.
- [51] G. Bellini, *et al.* Precision Measurement of the Be7 Solar

- Neutrino Interaction Rate in Borexino. *Physical Review Letters*, 107(1):141302, September 2011.
- [52] C. Arpesella, *et al.* Direct Measurement of the Be7 Solar Neutrino Flux with 192 Days of Borexino Data. *Physical Review Letters*, 101(9):91302, August 2008.
- [53] G. Bellini, *et al.* First Evidence of pep Solar Neutrinos by Direct Detection in Borexino. *Physical Review Letters*, 108(5):51302, February 2012.
- [54] B. Aharmim, *et al.* Measurement of the νe and total 8B solar neutrino fluxes with the Sudbury Neutrino Observatory phase-III data set. *Physical Review C*, 87(1):15502, January 2013.
- [55] B. Aharmim, *et al.* Determination of the νe and total B8 solar neutrino fluxes using the Sudbury Neutrino Observatory Phase I data set. *Physical Review C*, 75(4):45502, April 2007.
- [56] G. Bellini, *et al.* Measurement of the solar B8 neutrino rate with a liquid scintillator target and 3 MeV energy threshold in the Borexino detector. *Physical Review D*, 82(3):33006, August 2010.
- [57] K. Abe, *et al.* Solar neutrino results in Super-Kamiokande-III. *Physical Review D*, 83(5):52010, March 2011.
- [58] B. Aharmim, *et al.* Low-energy-threshold analysis of the Phase I and Phase II data sets of the Sudbury Neutrino Observatory. *Physical Review C*, 81(5):55504, May 2010.
- [59] S. N. Ahmed, *et al.* Measurement of the Total Active 8B Solar Neutrino Flux at the Sudbury Neutrino Observatory with Enhanced Neutral Current Sensitivity. *Physical Review Letters*, 92(1):181301, May 2004.
- [60] V. Berezinsky and M Lissia. Electron-neutrino survival probability from solar-neutrino data. *Physics Letters B*, 521(3):287–290, November 2001.
- [61] José Maneira. Status and Prospects of SNO+. *Nuclear Physics B - Proceedings Supplements*, 217(1):50–52, August 2011.
- [62] Michael Wurm, *et al.* The next-generation liquid-scintillator neutrino observatory LENA. *Astroparticle Physics*, 35(1):685–732, June 2012.